Talanta 135 (2015) 27–33

Contents lists available at ScienceDirect

Talanta

journal homepage: www.elsevier.com/locate/talanta

Enhancing reactive species generation upon photo-activation of CdTe quantum dots for the chemiluminometric determination of unreacted reagent in UV/$S_2O_8^{2-}$ drug degradation process

Rodolfo M.M. Santana [a], Thaís D. Oliveira [b], S. Sofia M. Rodrigues [c], Christian Frigerio [d], João L.M. Santos [c], Mauro Korn [e,*]

[a] Instituto de Química, Universidade Federal da Bahia, Rua Barão de Geremoabo Ferreira, 147, 40170-150 Salvador, Bahia, Brazil
[b] Universidade Federal de Juiz de Fora, Faculdade de Farmácia e Bioquímica, Rua José Lourenço Kelmer, s/n, 36036-900 Juiz de Fora, Minas Gerais, Brazil
[c] REQUIMTE, Departamento de Ciências Químicas, Faculdade de Farmácia, Universidade do Porto, Rua Jorge Viterbo Ferreira, 228, 4050-313 Porto, Portugal
[d] REQUIMTE, Departamento de Química e Bioquímica, Faculdade de Ciências, Universidade do Porto, Rua do Campo Alegre, 4169-007 Porto, Portugal
[e] Departamento de Ciências Exatas e da Terra, Universidade do Estado da Bahia, R. Silveira Martins, 2555, Cabula, 41195-001 Salvador, Bahia, Brazil

ARTICLE INFO

Article history:
Received 21 August 2014
Received in revised form
17 December 2014
Accepted 18 December 2014
Available online 29 December 2014

Keywords:
Multi-pumping flow system
CdTe
Quantum dots
Persulfate determination
Drug photo-chemical degradations

ABSTRACT

A new chemiluminescence (CL) flow method for persulfate determination was developed based on luminol oxidation by in-line generated radicals. Reactive oxygen species (ROS) generated by CdTe quantum dots (QDs) under a low energetic radiation (visible light emitted by LEDs) promoted the decomposition of persulfate ion ($S_2O_8^{2-}$) into sulfate radical ($SO_4^{\bullet-}$), leading to subsequent radical chain reactions that yield the emission of light. Due to the inherent radical short lifetimes and the transient behavior of CL phenomena an automated multi-pumping flow system (MPFS) was proposed to improve sample manipulation and reaction zone implementation ensuring reproducible analysis time and high sampling rate. The developed approach allowed up to 60 determinations per hour and determine $S_2O_8^{2-}$ concentrations between 0.1 and 1 mmol with good linearity (R=0.9999). The method has shown good repeatability with relative standard deviations below 2.5% (n=3) for different persulfate concentrations (0.1 and 0.625 mmol L^{-1}). Limits of detection (3σ) and quantification (10σ) were 2.7 and 9.1 μmol L^{-1}, respectively. The MPFS system was applied to persulfate determination in bench scale UV/$S_2O_8^{2-}$ drug degradation processes of model samples showing good versatility and providing real time information on the persulfate consumption in photo-chemical degradation methodologies.

1. Introduction

A fast population growth and a huge technological development have boosted drug production and consumption leading to the continuous introduction of significant amounts of pharmaceutical residues into the aquatic environment and their persistent occurrence in sewers and wastewater treatment plants. Some of these drugs, such as antibiotics, analgesic, anti-inflammatory, stimulants, steroids and β-blockers, are of great concern, not only because of their potential acute toxic effects but due to the long term chronic toxicity [1]. In addition, conventional water treatment processes cannot remove efficiently these emergent contaminants, as pharmaceuticals are generally intended not to be easily biodegradable and are often water soluble, which increases the bioaccumulation risks and potentiates the side effects on aquatic species and water consumers [2].

In this context, distinct non-biological methodologies have been proposed for effluent treatment aiming the elimination of these compounds, *e.g.* activated sludge [3], reverse osmosis [4], nanofiltration [5] and advanced oxidative processes (AOPs) [6]. AOPs are essentially based on the in-situ generation of highly reactive transitory species acting as mediators in the oxidative processes that promote the destruction of the target pollutants. Among these processes, Fenton's reactions and homogeneous or heterogeneous photocatalysis are the most popular ones and have demonstrated a great efficiency in degrading a wide range of organic persistent contaminants in water [7,8]. The photo-oxidative methods rely on the interaction of radiation (UV or visible light) with selected catalysts (TiO_2, Fe_2O_3, ZnO, *etc.*) or reagents (O_3, H_2O_2, $S_2O_8^{2-}$, *etc.*) to produce radical species that have strong oxidant activity. Recently, persulfate ($S_2O_8^{2-}$) has received special attention as an oxidant alternative for treating organic pollutants in waste [9] and

* Corresponding author.
E-mail address: mkorn@uneb.br (M. Korn).

http://dx.doi.org/10.1016/j.talanta.2014.12.021
0039-9140/

groundwater [10]. Upon thermal [11] or chemical [12] activation persulfate ion decomposes to produce sulfate free radicals ($SO_4^{\bullet -}$) which are powerful oxidants (E^0 between +2.5 and +3.1 V). The persulfate decomposition reaction [13] can be also induced by homolytic cleavage of peroxo bond under UV irradiation (Eq. (1)). The $SO_4^{\bullet -}$ high reactivity may initiate the generation of other oxidants species, since this radical can react with water molecules to produce $OH^{\bullet}$ radical (Eq. (2)), by a series of radical propagation and termination chain reactions that may lead to the formation of oxidant compounds such as H_2O_2, O_2 and HSO_5^- (Eqs. (3)–(5)), which increases the efficiency of the degradation of contaminants by UV/$S_2O_8^{2-}$ [13]. Several works have been developed employing these persulfate properties for the degradation of many drugs in water and wastewater treatment [14,15].

$$S_2O_8^{2-} + h\nu \rightarrow 2SO_4^{\bullet -} \quad (1)$$

$$SO_4^{\bullet -} + H_2O \rightarrow OH^{\bullet} + H^+ + SO_4^{2-} \quad (2)$$

$$SO_4^{\bullet -} + OH^{\bullet} \rightarrow HSO_5^- \quad (3)$$

$$2OH^{\bullet} \rightarrow H_2O_2 \quad (4)$$

$$S_2O_8^{2-} + H_2O_2 \rightarrow 2H^+ + 2SO_4^{2-} + O_2 \quad (5)$$

Owing to the growing number of UV/$S_2O_8^{2-}$ systems under application, the implementation of a straightforward and automated methodology to carry out the monitoring of persulfate during the whole treatment process would be a valuable asset as there is no available information about persulfate consumption in drug decomposition by UV/$S_2O_8^{2-}$ processes. This way it would be possible to survey the degradation progress, ensuring an adequate awareness of the reactions taking place and how they could be properly controlled, guaranteeing improved efficiency and the minimization of superfluous reagents and energy consumption. On the other hand, available methods for the quantification of persulfate are scarce and rely, almost exclusively, on spectrophotometric [16] and electrochemical [17] techniques.

Due to their unique optical properties [18], *e.g.* high quantum yield, resistance to photobleaching, symmetric narrow emission band and high absorption coefficient, light-emitting colloidal semiconductor nanocrystals or quantum dots (QDs), have been extensively investigated in distinct fields, namely as photodetectors [19], luminescent labels [20], and biosensing and bioimaging probes [21]. QDs were also found to generate light under an applied potential, being essential elements in many electrochemiluminescence applications [22].

A less exploited feature of quantum dots is their ability to generate reactive oxygen species (ROS) when exposed to ultraviolet, or even rarer, to visible light. Indeed, a low power light source emitting visible light can promote electrons from valence band (VB) to conduction band (CB) creating an exciton, a hole–electron pair (Eq. (6)), that can undergo redox reactions with surface adsorbed molecules. The hole–electron pair (h^+/e^-) redox properties depend mostly on the band-gap energy and bands edge [23].

For CdTe quantum dots band-gap energy is between 1.8 and 2.4 eV depending on nanocrystals size (redox potential of +0.94 V and −1.3 V for VB and CB, respectively) [24], that is potentially sufficient to reduce O_2 and to oxidize H_2O molecules to produce ROS [25], as shown in Eqs. (7) and (8). In this way, $S_2O_8^{2-}$ could react with specific ROS to create $SO_4^{\bullet -}$ radical, likewise the well known reaction between persulfate and Fe^{2+} (Eqs. (9) and (10)) [12].

$$2CdTe + h\nu \rightarrow CdTe(e_{CB}^-) + CdTe(h_{VB}^+) \quad (6)$$

$$CdTe(e_{CB}^-) + O_2 \rightarrow O_2^{\bullet -} \quad (7)$$

$$CdTe(h_{VB}^+) + H_2O \rightarrow CdTe + OH^{\bullet} + H^+ \quad (8)$$

$$S_2O_8^{2-} + O_2^{\bullet -} \rightarrow SO_4^{\bullet -} + SO_4^{2-} + O_2 \quad (9)$$

$$S_2O_8^{2-} + Fe^{2+} \rightarrow SO_4^{\bullet -} + SO_4^{2-} + Fe^{3+} \quad (10)$$

Although examined in the perspective of the cytotoxic effects in *in vivo* biological applications [26] or for photodynamic therapy [27], this interesting characteristic was seldom employed in analytical chemistry. For the best of our knowledge only a few analytical works have exploited ROS generation by QDs [28–30]. The reactivity of ROS could be combined with the advantageous analytical and operational characteristics of chemiluminescence methods such as simple instrumentation, high sensitivity, wide linear range and absence of background radiation interferences for the implementation of an automated methodology for persulfate determination.

The aim of this work was the development of a new analytical methodology, based on CdTe QDs photo-excitation with visible radiation, for persulfate determination, which was applied in bench scale UV/$S_2O_8^{2-}$ drug degradation processes. ROS generated by QDs were employed to react with $S_2O_8^{2-}$ inducing radical chain reactions. Luminol was applied as a probe for monitoring QD/$S_2O_8^{2-}$ radicals' production. Due to radical short lifetime and inherent transient behavior of CL signal a multi-pumping flow system was adopted to ensure analysis time reproducibility and high analytical throughput [31,32].

2. Experimental

2.1. Apparatus

The proposed flow system (Fig. 1) comprised five solenoid diaphragm-actuated micro-pumps (120SP, Bio-ChemValve Inc., Boonton, NJ, USA) with 10 μL of fixed internal volume. Micropumps were automatically controlled by microcomputer and activated by a homemade power drive connect to the computer by parallel port. The controlling program was developed in Visual Basic 6.0. Flow lines of PTFE with internal diameter of 0.8 mm and acrylic confluence points were employed to make the analytical pathway.

A bench scale photo-degradation unit (LUV) was built with a low pressure mercury lamp (Philips TUV 15W/G15T8) emitting UV radiation at 253.7 nm and a 200 cm PTFE reaction coil (0.8 mm i.d.). QDs activation for radicals' generation was accomplished in a home-made photo-excitation unit (LED-PEU) constituted by 50 cm PTFE reaction coil (0.8 mm i.d.) placed between two low power day-light led lamps (PARATHOM R50 40 D). The detection system was a chemiluminometer Plus FP-2020 Jasco (Easton, Maryland, USA) equipped with an helical flow cell with an internal volume of 100 μL that was

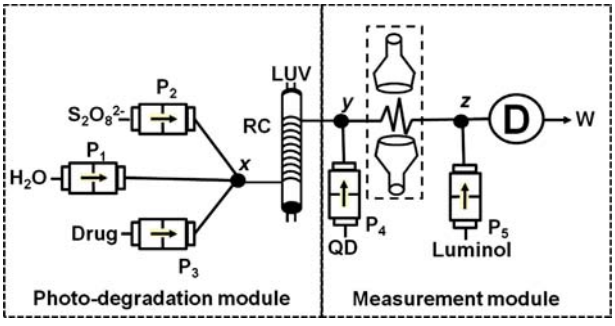

Fig. 1. Multi-pumping flow system (MPFS) for $S_2O_8^{2-}$ determination during drug degradation UV/$S_2O_8^{2-}$ processes. P_1–P_5: solenoid micro-pumps; *x*, *y* and *z*: confluence points; LUV: photo-degradation unit with UV lamp; RC: 200 cm reaction coil; LED-PEU: photo-excitation unit; D: chemiluminescence detector; W: waste.

positioned in front of a highly sensitive photomultiplier. A L250 E strip charted recorder (Linseis, Selb, Oberfranken, Germany) was adopted to record the CL analytical signals.

For nanocrystals characterization, atomic force microscopy (AFM) measurements were made using an AFM Workshop TTAFM instrument in vibrating (intermittent contact) mode. The UV/visible spectra of QDs solutions were recorded on a Jasco V-660 spectrophotometer UV–vis spectrometer between 400 and 700 nm. Nanocrystals X-ray powder diffraction (XRD) studies were carried out by using a Philips X'Pert X-ray MPD diffractometer (Cu Kα radiation). Fluorescence spectra were obtained with a PerkinElmer LS-50B luminescence spectrometer.

2.2. Solutions and standards

All solutions were prepared with deionized water and chemical reagents with analytical grade. A 5 mmol L^{-1} persulfate stock solution was prepared by dissolution of an appropriate amount of $K_2S_2O_8$ (Merck) in deionized water. Working persulfate solutions were prepared in the range between 0.1 and 1 mmol L^{-1} upon proper dilution of the referred $K_2S_2O_8$ stock solution. Model aqueous samples of disodium diclofenac, caffeine and amoxicillin, from Merck, at a concentration of 1 mmol L^{-1}, were used in the degradation studies. Luminol (Sigma-Aldrich) 10 mmol L^{-1} stock solution was prepared by dissolving appropriate amounts of the chemicals in basic medium (NaOH, 5 mmol L^{-1}) and kept under refrigeration and protect from light. A 2 mmol L^{-1} daily work solution was prepared by diluting the luminol stock solution. For quantum dots synthesis 5.0 mmol L^{-1} sodium borohydride (Sigma-Aldrich), 0.7 mmol L^{-1} tellurium powder (Sigma-Aldrich), 7.0 mmol L^{-1} cadmium chloride (Sigma-Aldrich) and 3.0 mmol L^{-1} of 3-mercaptopropionic acid (Fluka), were prepared. For the assays a 10.0 μmol L^{-1} aqueous solution of CdTe–MPA capped quantum dots, with a diameter of 3.7 nm, was daily prepared.

2.3. Quantum dots synthesis

Nanocrystals of CdTe capped with 3-mercaptopropionic acid (MPA) were synthesized by a hydrothermal method following the procedure previously proposed by Silvestre et al. [33] and Zou et al. [34]: tellurium precursor, a NaHTe solution, was obtained upon reaction of Te powder with $NaBH_4$, in N_2 saturated water. NaHTe was subsequently transferred into a second flask containing 4.0 mmol of $CdCl_2$ (cadmium precursor) and 6.8 mmol of MPA, in a 100 mL N_2 saturated solution. The molar ratio of Cd^{2+}:Te^{2-}:MPA was fixed at 1:0.1:1.7. The solution pH was adjusted to 11.5 by addition of 1 mol L^{-1} NaOH.

The obtained QDs were purified by precipitation and fractioning with ethanol. The precipitate fractions were subsequently washed with ethanol, centrifuged and vacuum dried. All the fractions obtained were re-suspended in water maintaining the initial synthesis concentration. Working solutions were daily prepared by suitable dilution with water.

2.4. Quantum dots characterization

CdTe nanocrystals with distinct sizes, ranging from 2.3 to 3.7 nm, were prepared by changing the synthesis refluxing time. The population of QDs obtained for each particular synthesis was very homogeneous with a circumscribed size distribution, as confirmed by the narrow fluorescence emission bands obtained, with Full Width at Half Maximum (FWHM) values in the range from 41 to 47 nm. The typically broad absorption spectra exhibited a well-defined peak corresponding to the first excitonic transition. The wavelength of this first transition (λ) was used in the estimation of the nanocrystals diameter (D), expressed in nm, according to the equation proposed by Yu et al. [35]:

$$D = \left(9.8127 \times 10^{-7}\right)\lambda^3 - \left(1.7147 \times 10^{-3}\right)\lambda^2 + (1.0064)\lambda - (194.84) \quad (11)$$

Aiming at standardizing the concentration of all CdTe QDs solutions, the extinction coefficient (ε) of the quantum dots of a given diameter (D), was calculated according to the following expression:

$$\varepsilon = 3450 \times \Delta E \times (D)^{2.4} \quad (12)$$

where ΔE is the transition energy expressed in eV which corresponds to the first excitonic transition. Upon knowing ε and by measuring the absorbance of a solution with a known mass of QDs, the molar concentration was calculated by applying Lambert–Beer's law.

2.5. Flow procedure

The proposed flow system had two modules (Fig. 1); the first one was a photo-degradation module (LUV), where the model drug was mixed with $S_2O_8^{2-}$ and exposed to UV radiation, and the second module was a measurement unit used to quantify the persulfate in solution. In the case of the drug degradation assays it allowed quantification of the remaining persulfate. The analytical cycle (Table 1) began with the simultaneous insertion of 160 μL of persulfate and model drug into the LUV (Steps 1 and 2); subsequently the flow was stopped to allow exposure of the sample zone to UV radiation for time intervals between 5 and 60 s (Step 3); then, the sample zone (containing an unknown amount of persulfate) was carried towards the confluence x and mixed with 80 μL of QDs (Steps 4 and 5) creating a reaction zone that was propelled through the LED-PEU unit for radicals generation (Step 6); finally, the referred reaction zone was promptly mixed with 20 μL of luminol (step 7) and immediately sent to the detector for measurement (Step 8).

2.6. Chromatographic analysis

Drug degradation efficiency was evaluated by measuring the amount of drug remaining in solution after treatment. This was accomplished by liquid chromatography according to the United States Pharmacopeia recommendations [36]. Immediately after the LUV module an aliquot of the solution was collected and analyzed for concentration assessment of each of the studied model drugs.

The assays were performed in a HPLC M Merck/Hitachi – LaChrom 7000 (Schaumburg, Illinois, USA) with diode array detector (DAD L-7100) and manual injector Rheodyne 7725i (20 μL). Chromatographic analysis was achieved in isocratic mode during 15 min for all model species. The columns adopted were Chromolith RP-18e (ID 250 × 4.6 mm) for caffeine and amoxicillin and Chromolith RP-8e (ID 100 × 4.6 mm) for sodium diclofenac. A guard column (ID 5.0 × 4.6 mm) was used for caffeine and diclofenac analysis. Different mobile phases were employed: (i) for amoxicillin

Table 1
Analytical cycle used for drug degradation and determination of persulfate in multi-pumping flow system.

Step	Description	Pump	Pulses	Time (ms)
1	$K_2S_2O_8$ and drug insertion	P_2+P_3	8	300
2	Transport to LUV	P_1	30	300
3	Photo degradation	P_1	0	Variable
4	Transport to confluence x	P_1	45	300
5	QDs insertion	P_4	8	300
6	Transport through LED-PEU unit	P_1	30	800
7	Luminol insertion	P_5	2	300
8	Signal acquisition	P_1	45	200

the eluent consisted in acetonitrile/KH_2PO_4 (4:96) solution at 5.0 pH with flow rate of 1.5 mL min^{-1}; (ii) caffeine's eluent was acetonitrile/tetrahydrofuran/sodium acetate (2.5:2:95.5) at 4.5 pH with flow rate of 1.0 mL min^{-1}; and (iii) methanol/phosphate buffer solution (73:27) at 2.5 pH with flow rate of 1.0 mL min^{-1} was used for diclofenac determinations. Detector was set at 230, 275 and 254 nm for amoxicillin, caffeine and diclofenac determinations, respectively.

3. Results and discussion

The photo-irradiation of solutions combining $S_2O_8^{2-}$ and CdTe–MPA capped quantum dots within a Multi-Pumping Flow System triggered the intense generation of reactive species capable of oxidizing luminol with the concomitant emission of light. The mixing of the two compounds had a synergistic effect as the intensity of emitted light was much higher when they were combined than when they were individually irradiated (for comparative purposes, in the latter case was considered the sum of the intensities of light emitted by the individual solutions). Light intensity was affected by several chemical and operational parameters.

3.1. System optimization

The optimization of chemical and physical MPFS parameters was performed by using an univariate model and aimed at the best analytical response. In the first assays it was confirmed the effect QDs size on free radical generation, and that this parameter played an important role in the radical chain reaction. Therefore, in a first stage, QDs size effect on analytical signal was evaluated by using four different sized MPA–CdTe QDs (2.3, 2.9, 3.2 and 3.7 nm). The analytical signals provided by photo-excitation of a combined solution of $S_2O_8^{2-}$ and QDs were compared to those furnished by isolated solutions of the two compounds. Starting from quantum dots of 2.9 nm, the results showed (Fig. 2a) that by increasing QDs size a significant enhancement of the chemiluminescence reaction was attained (ca. 280% regarding the sum of the signals produced by individual $S_2O_8^{2-}$ and QDs solutions) for 3.7 nm nanocrystals. This observation was in agreement with Ribeiro et al. [28], whom confirmed improved ROS yield production for largest nanomaterials. This synergistic effect between persulfate and the QDs may be explained by the occurrence of direct or indirect radical reactions that lead to the production of strong oxidant species, such as those above mentioned (i.e. H_2O_2, HSO_5^- and O_2), which promoted the oxidation of luminol to 3-aminophthalate.

Another important parameter affecting analytical response was the QDs concentration, which was studied in the range between 0.5 and 10 μmol L^{-1} (Fig. 2b). For a 10 μmol L^{-1} solution a pronounced increasing in light emission, of about 150% regarding the lowest concentration tested, was observed. These results confirmed the direct relationship between the nanocrystals concentration in solution, subject to irradiation, and the amount of ROS produced. Consequently, for the succeeding optimization assays 3.7 nm QDs in 10 μmol L^{-1} concentration were selected.

Although not directly related with radical generation, luminol and NaOH concentration also had an important influence in the extension of the chemiluminescence reaction that led to light emission. The influence of luminol concentration was investigated from 0.1 up to 2.0 mmol L^{-1} and it was observed a rising, almost linear relationship between CL intensity and luminol (Fig. 2c). On the contrary, there was no significant variation in the CL signal for the NaOH concentrations tested (5–100 mmol L^{-1}) (Fig. 2d). Accordingly, and as a compromise between sensitivity and reagents consumption, a 2.0 mmol L^{-1} luminol solution prepared in 5 mmol L^{-1} NaOH was adopted for the analysis.

The irradiation time during the photo-excitation step was a *sine qua non* parameter since ROS production depends on it. Increased irradiation times could be achieved either be using lower flow rates or by halting the sample zone under the light source for a given period of time. However, since halting the flowing stream impaired reaction zone homogenization, as reagents mixing do not take place in a stopped flow, the latter option was more prone to poorer signal reproducibility. In view of that, exposure time was evaluated by varying the carrier flow rate from 4.7 to 28.6 μL min^{-1} (Fig. 3a). The obtained results showed that the analytical signals were affected not only by the irradiation time but also by the short lifetime of the generated radicals. Indeed, at the lowest flow rates QDs were subjected to an increased irradiation, but, at the same time the radical resident time in the analytical pathway also increased, which favored the occurrence of radical deactivation reactions. For this reason, the lowest flow rates did not produce the highest signals. On another hand, the highest flow rates led to the smallest response since QDs were inadequately exposed to radiation: CL signal decayed about 35% for flow rates greater than 10.5 μL min^{-1}. In accordance, a flow rate of 8.7 μL min^{-1} that better conciliated these two opposing effects (formation and deactivation of radical), was selected for the assays.

The magnitude of the flow rate that determined the transport of the reaction zone towards detection, immediately after luminol insertion, was also evaluated because of the transient behavior of CL emission and the high reaction kinetics of luminol (Fig. 3b). Flow rates between 4.7 and 28.6 μL min^{-1} were examined and no significant difference was observed in the analytical response. This could be probably explained by the reduced length of the tubing placed between confluence *z* and the detector, which however did not affect the mixture and consequently the reproducibility. For improved sample throughput, without compromising sensitivity, a 28.6 μL min^{-1} flow rate was selected for samples measurement.

3.2. Analytical features

Under optimal conditions the MPFS system allowed 60 determinations per hour with low waste generation (1.3 mL h^{-1}) and low reagent consumption (0.44 and 32.0 mg of luminol and QDs were consumed per hour, respectively). Linear working range was observed ($R=0.9999$) for persulfate concentrations between 0.1 and 1 mmol L^{-1}. The developed method has shown good repeatability, with relative standard deviations lower than 2.5% ($n=3$) for 0.1 and 0.625 mmol L^{-1} persulfate concentrations. For reference solution with persulfate concentration of 0.1 mmol L^{-1} it was calculated concentration mean of 0.107 ± 0.002 mmol L^{-1}, while for reference solution of 0.625 mmol L^{-1} persulfate the mean calculated for persulfate concentration by the calibration curve was 0.668 ± 0.014 mmol L^{-1}. Additionally, good sensitivity with limits of detection (3σ) and quantification (10σ) of about 2.7 and 9.1 μmol L^{-1} were respectively estimated.

The analytical features provided by this methodology are quite similar to those referred in previous works dealing with persulfate determination (Table 2), but the proposed approach assured a substantial decrease in reagent consumption and waste generation without affecting analytical performance and efficiency. In addition, the developed automated flow system could be easily set-up to assure real time continuous monitoring of persulfate content during advanced oxidation processes in, for instances, water treatment plants.

3.3. Persulfate consumption and drug degradation

To evaluate the performance of the developed approach the bench scale degradation system was applied in the treatment of control samples individually spiked with the target drugs previously

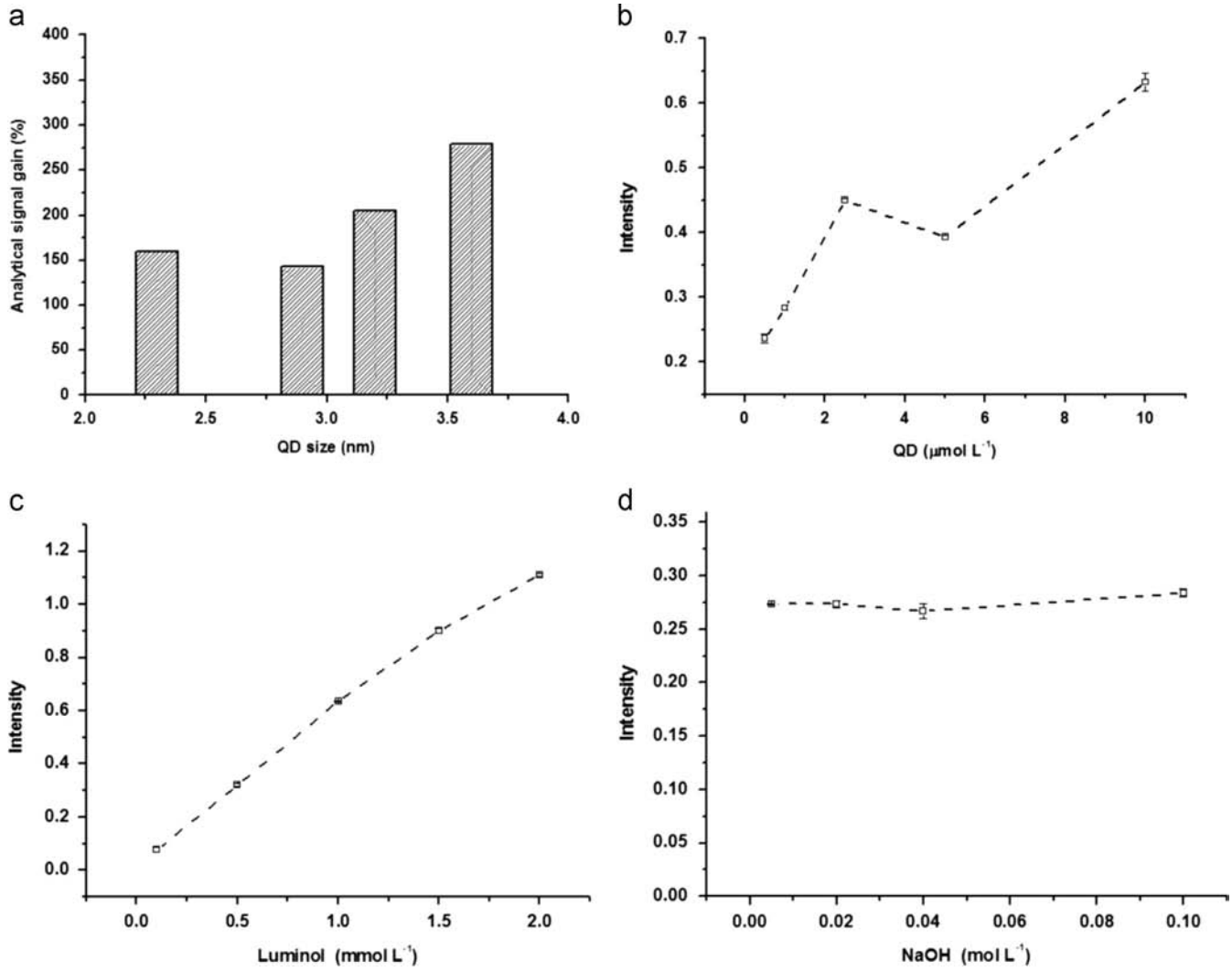

Fig. 2. Influence of chemical parameters on analytical signal in multi-pumping flow system: (a) QD size; (b) QD concentration; (c) luminol concentration; and (d) NaOH concentration.

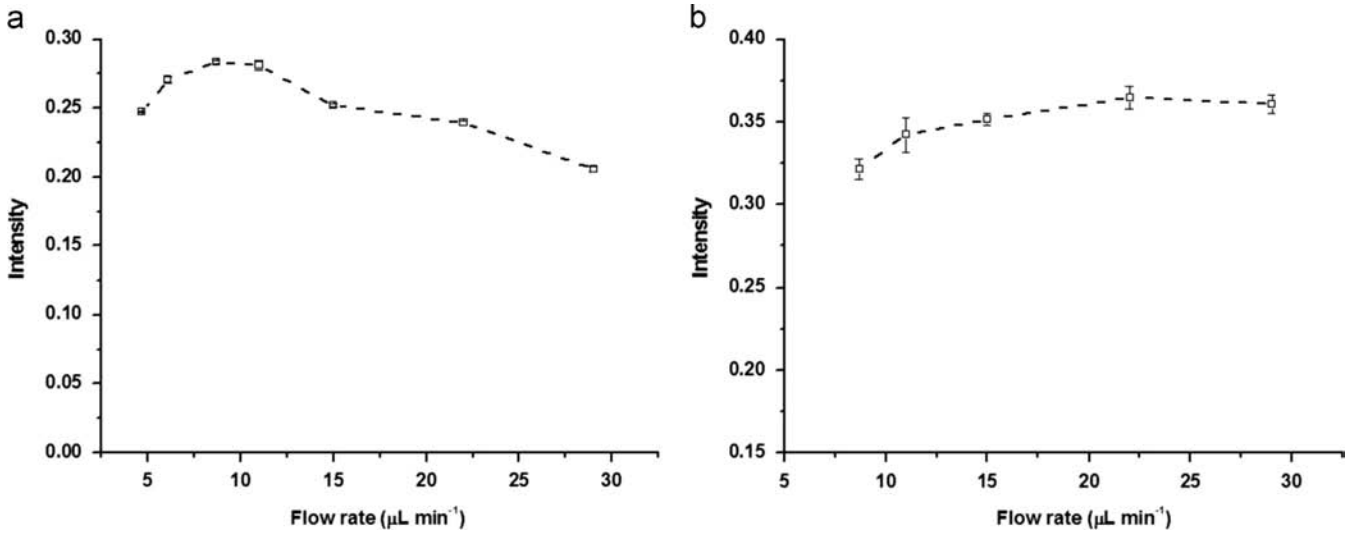

Fig. 3. Influence of physical parameters on analytical signal in MPFS system: (a) flow rate during the photo-excitation of QD/$S_2O_8^{2-}$ zone and (b) flow rate during the transport of the reaction zone to detector.

mentioned. The persulfate concentration were always in excess and their consumption profiles were similar, regardless of the drug submitted to degradation: in the beginning of the process about 25% of persulfate were immediately consumed, followed by a moderate consumption until conclusion. The total amount of $S_2O_8^{2-}$ spent during the whole process was between 45 and 60%.

Table 2
Analytical features of some methods employed for persulfate determination.

Sample	Technique	LOD (μmol L^{-1})	Linear range (μmol L^{-1})	RSD (%)	Reference
Inorganic model sample	Ion chromatography	0.9	216–8220	< 5.0	[37]
n.i.	Amperometry	0.3	0.1–12,000		[17]
n.i.	Amperometry	1.0	10–100; 3100–101,000	n.i.	[38]
Cosmetic products	Flow-amperometry	90.0	100–1000	2.2	[39]
Spiked wastewater	Spectrophotometry	0.42	2.0–100	n.i.	[40]
Spiked wastewater	Flow-chemiluminescence	2.7	100–1000	< 2.5	This work

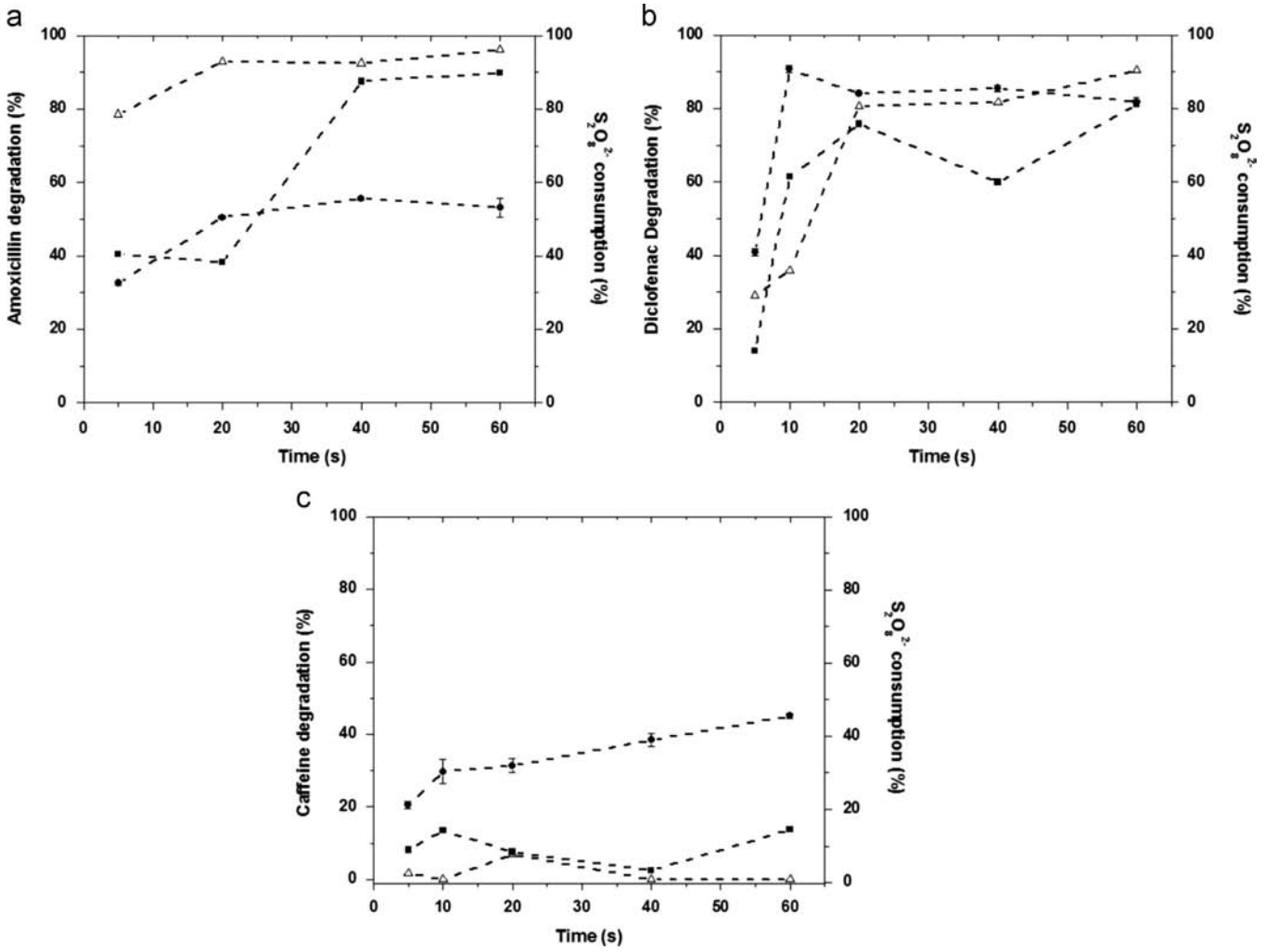

Fig. 4. Results obtained after drugs degradation in a bench scale photo-reactor. Persulfate consumption profile (–•–); Degradation of amoxicillin (a), diclofenac (b), caffeine (c) 1.0 mmol L^{-1} solutions under UV irradiation (–Δ–) and UV/$S_2O_8^{2-}$ (–■–).

On the other hand, the efficiency of UV/$S_2O_8^{2-}$ process was markedly different for each drug degradation: caffeine has shown a recalcitrant behavior and was poorly degraded (only 20% of this drug was oxidized after 60 s), while under the same conditions more than 90% of amoxicillin and diclofenac were decomposed. To assess the effective contribution of persulfate in UV/$S_2O_8^{2-}$ process the drugs were submitted exclusively to UV radiation, without the reagent. The results demonstrated that during the early stages the UV radiation was more efficient for amoxicillin and diclofenac degradation than the combination UV/$S_2O_8^{2-}$ (Fig. 4a and b). This could be explained by the fact that in this situation (only UV) drug molecules absorbed UV radiation that had sufficient energy for the drug abatement, but with UV/$S_2O_8^{2-}$ the persulfate also absorbed UV radiation, which promoted the breaking down of O–O bond producing $SO_4^{\bullet-}$ radical, decreasing the energy available for the drug degradation process. However, in the end both procedures reached the same degradation level and there was no significant difference whether $S_2O_8^{2-}$ was used or not. Caffeine was also resilient to UV radiation alone, but in despite of this recalcitrant behavior when persulfate was used better results were achieved (Fig. 4c).

4. Conclusions

The combined irradiation of $S_2O_8^{2-}$ and CdTe–MPA capped QDs with a low power white LED light demonstrated to be able to intensively promote the generation of reactive species that could trigger the decomposition of persulfate into $SO_4^{\bullet-}$ radical. This was capable of oxidizing luminol with the concomitant concentration related emission of light that was used to assess persulfate

concentration. CdTe QDs photo-activation was size dependent being radical generation more pronounced for the biggest nanocrystals. The implementation of the developed reactional scheme by using a multi-pumping flow system showed the capacity to determine persulfate with both good precision and accuracy, providing low detection and quantification limits and high sampling rate and enabling reagents saving and the minimization of waste generation.

Acknowledgments

Rodolfo M.M. Santana thanks the "Coordenação de Aperfeiçoamento de Pessoal de Ensino Superior" of Brazilian Education Ministery for the Ph.D. fellowship. S. Sofia M. Rodrigues thanks the "Fundação para a Ciência e Tecnologia" and FSE (Quadro Comunitário de Apoio) for the Ph.D. Grant (SFRH/BD/70444/2010). All authors are grateful to support from Brazil (CAPES) – Portugal (FCT) bilateral scientific cooperation project.

References

[1] I. Sirés, E. Brillas, Environ. Int. 40 (2012) 212–229.
[2] K. Kümmerer, J. Environ. Manage. 90 (2009) 2354–2366.
[3] O.A.H. Jones, N. Voulvoulis, J.N. Lester, Environ. Pollut. 145 (2007) 738–744.
[4] J.H. Al-Rifai, H. Khabbaz, A.I. Schäfer, Sep. Purif. Technol. 77 (2011) 60–67.
[5] F. Zaviska, P. Drogui, A. Grasmick, A. Azais, M. Héran, J. Membr. Sci. 429 (2013) 121–129.
[6] M. Klavarioti, D. Mantzavinos, D. Kassinos, Environ. Int. 35 (2009) 402–417.
[7] E. Neyens, J. Baeyens, J. Hazard. Mater. 98 (2003) 33–50.
[8] M.N. Chong, B. Jin, C.W.K. Chow, C. Saint, Water Res. 44 (2010) 2997–3027.
[9] Y. Shiying, W. Ping, Y. Xin, W. Guang, Z. Weny, S. Liang, J. Environ. Sci. 21 (2009) 1175–1180.
[10] R.J. Watts, A.L. Teel, Pract. Period. Hazard. Toxic, Radioact. Waste Manage. 10 (2006) 2–9.
[11] V.C. Mora, J.A. Rosso, G.C. Le Roux, D.O. Mártire, M.C. Gonzalez, Chemosphere 75 (2009) 1405–1409.
[12] G.P. Anipsitakis, D.D. Dionysiou, Environ. Sci. Technol. 38 (2004) 3705–3712.
[13] H. Hori, A. Yamamoto, K. Koike, S. Kutsuna, I. Osaka, R. Arakawa, Water Res. 41 (2007) 2962–2968.
[14] Y. Gao, N. Gao, Y. Deng, Y. Yang, Y. Ma, Chem. Eng. J. 195 (2012) 248–253.
[15] C. Tan, N. Gao, Y. Deng, Y. Zhang, M. Sui, J. Deng, S. Zhou, J. Hazard. Mater. 260 (2013) 1008–1016.
[16] C. Liang, C. Huang, N. Mohanty, R.M. Kurakalva, Chemosphere 73 (2008) 1540–1543.
[17] Z. Savari, S. Soltanian, A. Noorbakhsh, A. Salimi, M. Najafi, P. Servati, Sens. Actuators B 176 (2013) 335–343.
[18] A.P. Alivisatos, J. Phys. Chem. 100 (1996) 13226–13239.
[19] P. Bhattacharya, S. Ghosh, A.D. Stiff-Roberts, Annu. Rev. Mater. Res. 34 (2004) 1–40.
[20] X. Michalet, F.F. Pinaud, L.A. Bentolila, J.M. Tsay, S. Doose, J.J. Li, G. Sundaresan, A.M. Wu, S.S. Gambhir, S. Weiss, Science 307 (2005) 538–544.
[21] J.M. Klostranec, W.C. Chan, Adv. Mater. 18 (2006) 1953–1964.
[22] C. Frigerio, D.S.M. Ribeiro, S.S.M. Rodrigues, V.L.R.G. Abreu, J.A.C. Barbosa, J.A.V. Prior, K.L. Marques, J.L.M. Santos, Anal. Chim. Acta 735 (2012) 9–22.
[23] B.I. Ipe, M. Lehnig, C.M. Niemeyer, Small 7 (2005) 706–709.
[24] G.P. Kissling, D.J. Fermin, Phys. Chem. Chem. Phys. 11 (2009) 10080–10086.
[25] M.V. Kovalenko, M.I. Bodnarchuk, A.L. Stroyuk, S.Y. Kuchmii, Theor. Exp. Chem. 40 (2004) 220–225.
[26] A.M. Derfus, W.C.W. Chan, S.N. Bhatia, Nano Lett. 4 (2004) 11–18.
[27] A.C.S. Samia, X. Chen, C. Burda, J. Am. Chem. Soc. 125 (2003) 15736–15737.
[28] D.S.M. Ribeiro, C. Frigerio, J.L.M. Santos, J.A.V. Prior, Anal. Chim. Acta 735 (2012) 69–75.
[29] C.P. Huang, Y.K. Li, T.M. Chen, J. Nanosci. Nanotechnol. 8 (2008) 3434–3438.
[30] W.J. Jin, M.T. Fernandez-Arguelles, J.M. Costa-Fernandez, R. Pereiro, A. Sanz-Medel, Chem. Commun. 7 (2005) 883–885.
[31] J.L.M. Santos, M.F.T. Ribeiro, A.C.B. Dias, J.L.F.C. Lima, E.E.A. Zagatto, Anal. Chim. Acta 600 (2007) 21–28.
[32] M.F.T. Ribeiro, J.L.M. Santos, J.L.F.C. Lima, Anal. Chim. Acta 600 (2007) 14–20.
[33] C.I.C. Silvestre, C. Frigerio, J.L.M. Santos, J.L.F.C. Lima, Anal. Chim. Acta 699 (2011) 193–197.
[34] L. Zou, Z. Gu, N. Zhang, Y.Z. Fang, W. Zhu, X. Zhong, J. Mater. Chem. 18 (2008) 2807–2815.
[35] W.W. Yu, L. Qu, W. Guo, X. Peng, Chem. Mater. 15 (2003) 2854–2860.
[36] United States Pharmacopeia and National Formulary – USP 32 NF27, US Pharmacopoeial Convention, Rockville, 2009.
[37] N.E. Khan, Y.G. Adewuyi, J. Chromatogr. A 1218 (2011) 392–397.
[38] K.C. Lin, J.Y. Huang, S.M. Chen, Int. J. Electrochem. Sci. 7 (2012) 9161–9173.
[39] M.F. De Oliveira, A.A. Saczk, J.A.G. Neto, P.S. Roldan, N.R. Stradiotto, Sensors 3 (2003) 371–380.
[40] Y. Ding, L. Zhu, J. Yan, Q. Xiang, H. Tang, J. Environ. Monit. 13 (2011) 3057–3063.